Proc. Natl. Acad. Sci. USA
Vol. 92, pp. 10658–10662, November 1995
Neurobiology

An alternative pathway for signal flow from rod photoreceptors to ganglion cells in mammalian retina

(gap junction/2-amino-4-phosphonobutyric acid/bipolar cell/multielectrode recording)

STEVEN H. DEVRIES† AND DENIS A. BAYLOR

Department of Neurobiology, Sherman Fairchild Science Building, Stanford University Medical School, Stanford, CA 94305

Contributed by Denis A. Baylor, August 16, 1995

ABSTRACT **Rod signals in the mammalian retina are thought to reach ganglion cells over the circuit rod → rod depolarizing bipolar cell → AII amacrine cell → cone bipolar cells → ganglion cells. A possible alternative pathway involves gap junctions linking the rods and cones, the circuit being rod → cone → cone bipolar cells → ganglion cells. It is not clear whether this second pathway indeed relays rod signals to ganglion cells. We studied signal flow in the isolated rabbit retina with a multielectrode array, which allows the activity of many identified ganglion cells to be observed simultaneously while the preparation is stimulated with light and/or exposed to drugs. When transmission between rods and rod depolarizing bipolar cells was blocked by the glutamate agonist 2-amino-4-phosphonobutyric acid (APB), rod input to all On-center and briskly responding Off-center ganglion cells was dramatically reduced as expected. Off responses persisted, however, in Off-center sluggish and On–Off direction-selective ganglion cells. Presumably these responses were generated by the alternative pathway involving rod–cone junctions. This APB-resistant pathway may carry the major rod input to Off-center sluggish and On–Off direction-selective ganglion cells.**

Rod input to ganglion cells in the mammalian retina is usually assumed to flow over the circuit shown in Fig. 1. Rod depolarizing bipolar (RDB) cells carry amplified, sign-inverted rod signals to AII amacrine cells. Gap junctions then relay the light-evoked depolarization from AII amacrine cells to cone depolarizing bipolar cells, which in turn excite On-center ganglion cells. Depolarizing rod signals in AII amacrine cells also release inhibitory transmitter onto the cone hyperpolarizing bipolar cells, which provide excitatory drive to Off-center ganglion cells (1–4). Physiological observations support the key role of RDB cells in this circuit. For example, the glutamate agonist 2-amino-4-phosphonobutyric acid (APB), which acts on metabotropic receptors to interrupt transmission between photoreceptors and depolarizing bipolar cells (5–7), reportedly blocks rod-mediated responses of both On- and Off-center ganglion cells and cone-mediated responses of On-center ganglion cells (1, 8). Cone-mediated responses of Off-center ganglion cells survive APB because it does not block transmission from cones to cone hyperpolarizing bipolar cells (1, 5).

Rods and ganglion cells might be linked by an alternative pathway. Anatomical observations (9, 10) and recordings from neurons in the outer retina (11–14) indicate that rod signals may spread to cones through gap junctions. Rod signals that reached cones via these junctions might then flow to ganglion cells over cone bipolar cells, bypassing RDB and AII amacrine cells. Although psychophysical measurements (15, 16) have suggested that rod signals may travel in two pathways with different sensitivity and kinetics, there is no evidence up to now that rod signals can drive ganglion cells over the alternative pathway.

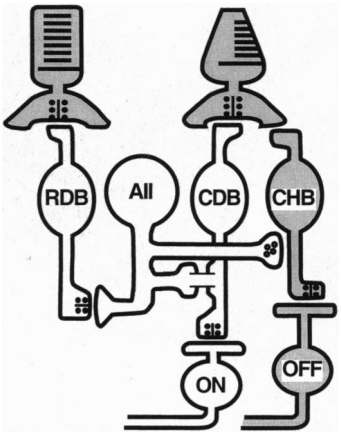

FIG. 1. Simplified diagram of pathways connecting photoreceptors and ganglion cells in mammalian retina. Neurons that depolarize in light are shown in white and those that hyperpolarize are shaded. AII amacrine cells are depolarized by sign-preserving input from RDB cells. AIIs make sign-preserving electrical connections onto cone depolarizing bipolar (CDB) cells and sign-reversing glycinergic (inhibitory) connections onto cone hyperpolarizing bipolar (CHB) cells. On- and Off-center ganglion cells are shown.

We made multielectrode recordings (17) from ganglion cells in the isolated rabbit retina in an attempt to evaluate the functional contribution of the alternative pathway. APB was used to block transmission in the classical pathway, and rod and cone inputs were distinguished by their characteristic spectral properties. Evidence was obtained that rod signals indeed reach ganglion cells over the alternative pathway and that this pathway provides the predominant link between rods and ganglion cells of the Off-center sluggish and On–Off direction-selective (On–Off DS) types.

MATERIALS AND METHODS

Preparation and Recording. Rabbits (pigmented New Zealand White; 12–20 weeks old) were maintained in the dark overnight and sacrificed in accordance with institutional guidelines by an i.v. overdose of pentobarbital. Eyes were enucleated and the posterior pole was cleared of vitreous under dim red light with an infrared-to-visible image converter. The eyecup was bathed in Hepes-buffered Ames medium (Sigma, catalogue no. A1420; supplemented with 10 mM Hepes buffer/15 mM NaCl, pH 7.35) and a portion (4 × 4 mm) of central retina was peeled from the pigment epithelium with fine forceps. The retina was placed ganglion cell side down on a multielectrode array, where it was held in place by a piece of taut dialysis

The publication costs of this article were defrayed in part by page charge payment. This article must therefore be hereby marked "*advertisement*" in accordance with 18 U.S.C. §1734 solely to indicate this fact.

Abbreviations: APB, 2-amino-4-phosphonobutyric acid; RDB, rod depolarizing bipolar; On–Off DS cell, On–Off direction-selective cell.

†To whom reprint requests should be addressed.

membrane. It was superfused continuously at a rate of 0.5 ml/min with bicarbonate-buffered Ames medium (34–35°C), which was preequilibrated with 5% CO_2/95% O_2. Solution pH was 7.35.

Multielectrode recordings from the isolated retina were made as described (17). The multielectrode array consisted of 61 extracellular platinum electrodes lying on a planar glass substrate in a hexagonal pattern, 545 μm wide. The spacing between neighboring electrodes was 60 μm and the electrode diameter was 20 μm. Voltage signals at the electrodes were conducted to amplifiers by indium tin oxide leads insulated from the Ames medium by a thin layer of polyimide plastic. The voltage at each electrode was continuously monitored by a peak detector circuit that measured the peak amplitude, time of occurrence, and duration of events that exceeded a selectable threshold. These values were stored in a Macintosh computer for off-line analysis.

Characterization of Receptive Fields. Ganglion cell receptive fields were determined as described (17, 18). A checkerboard pattern generated by a Macintosh high-resolution RGB color monitor was imaged on the retinal surface by a microscope objective. Usually, each square of the checkerboard was made green or black according to a pseudorandom sequence and the entire pattern was updated continuously at 13.3 or 16.7 Hz. In some experiments, receptive fields were characterized with a polychromatic checkerboard in which the color of each square was selected by activating the red, green, and blue phosphors in the monitor randomly and independently. One square was 94 or 104 μm wide. The mean stimulus intensity was adjusted by neutral density filters in the light path and monitor controls. Experimental runs lasted a minimum of 20 min. At the end of an experiment, spikes recorded by each electrode were sorted into the activity of individual neurons. Each neuron's spike train was then cross-correlated with the sequence of checkerboard patterns projected onto the retina, yielding the cell's spike-triggered average stimulus. This is the stimulus, a function of space and time, that on average preceded the occurrence of a spike. The spike-triggered average stimulus has units of light intensity. Plots of normalized intensity vs. time were obtained by averaging the stimulus intensity over squares in the center of a receptive field, selecting squares if their intensity exceeded a value that would rarely occur by chance.

Calibration of Light Stimuli. Light stimuli were generated by the Macintosh monitor or by a conventional stimulator with a tungsten iodide source (19). Rod photoisomerization rates were calculated from stimulus intensities measured at the level of the retinal surface with a calibrated radiometric photodiode (United Detector Technologies, Santa Monica, CA). Light from the tungsten bulb was bandpass filtered (501-nm peak, 10-nm half-bandwidth interference filter) and the power at the photodiode was converted directly to 501-nm photon flux. For calibrating the intensities of each phosphor of the Macintosh color monitor, the power of incident light measured with the photodiode was used to scale the emission spectrum of each phosphor, measured by a spectrophotometer [EG&G Gamma Scientific, San Diego (17)], so that the wavelength integral of the phosphor's emission spectrum was equal to the power measured by the photodiode. The photon flux at each wavelength was then calculated.

The fraction of incident light absorbed by rhodopsin in the rods was measured at the end of each experiment. A spot of 501-nm light (10-nm half-bandwidth) was focused on the retinal surface in the region overlying the multielectrode array. The intensity transmitted by the retina and array was measured by a photomultiplier (Princeton Applied Research, model 1140A) before and after a 10-min exposure to intense white bleaching light. The fraction of incident light, A, absorbed by the pigment during the experiment was found from $A = (1 - i_o/i_{bl})$ where i_o and i_{bl} are the transmitted intensities measured before and after bleaching, respectively. Cone absorption was neglected since cones make up <5% of the photoreceptor population. Determined in this way, the fraction of incident light absorbed was usually near 0.2.

Photon flux density was converted to mean photoisomerization rate per rod ($Rh^*{\cdot}rod^{-1}{\cdot}s^{-1}$). For the tungsten beam, $Rh^*{\cdot}rod^{-1}{\cdot}s^{-1}$ was calculated from the expression $Rh^*{\cdot}rod^{-1}{\cdot}s^{-1} = A \times I \times 0.67/r_D$, where I is the photon flux density of the 501-nm light at the retina, 0.67 is the quantum efficiency of photoisomerization, and r_D is the rod density, taken as 240,000 mm^{-2} in the central portion of the retina just inferior to the visual streak (4). For each phosphor in the color monitor, $Rh^*{\cdot}rod^{-1}{\cdot}s^{-1}$ was determined by multiplying pointwise the scaled emission spectrum and the rod absorption spectrum (20) normalized to a value of 0.2 at 501 nm, integrating over wavelength, and correcting for the quantum efficiency of photoisomerization and the rod density.

The relative efficiencies with which different photopigments were stimulated by each monitor gun were calculated by multiplying at each wavelength the normalized pigment absorption spectrum [blue cone λ_{max} = 430 nm; green cone λ_{max} = 530 nm (21); rod λ_{max} = 500 nm (20)] by the scaled emission spectrum of the phosphor and comparing the integrals over wavelength. At the retinal surface, the unattenuated light intensity from each phosphor was 6.91×10^{-15} $W{\cdot}\mu m^{-2}$ (blue), 6.63×10^{-15} $W{\cdot}\mu m^{-2}$ (green), and 5.53×10^{-15} $W{\cdot}\mu m^{-2}$ (red).

RESULTS

With the multielectrode array (17, 22), it was possible to monitor simultaneously the responses of up to 80 rabbit ganglion cells and to observe the effects of APB on their receptive fields. Fig. 2*A* illustrates receptive fields measured in control and APB-containing solutions, using a very dim stimulus that should have effectively activated only rods. APB (40 μM) blocked responses in the On-center ganglion cell, as expected, and the measured receptive field became structureless. A similar block occurred in each of eight On-center ganglion cells in this retina. Surprisingly, responses persisted in the cells illustrated in Fig. 2 *B* and *C*. The cell in Fig. 2*B* was identified as an On–Off DS cell on the basis of its responses to drifting sinewave gratings (23). Cells of this type comprised ≈25% of recorded ganglion cells (see also ref. 24). The spike-triggered average stimulus of the On–Off DS cell in Fig. 2*B* was a darkening over the field center, suggesting that the Off mechanism of this type of ganglion cell was more powerful at the low stimulus intensity used. APB had little effect on the cell's receptive field, and a similar lack of effect was observed in each of 56 On–Off DS cells in nine retinas. APB also had little effect on the receptive field of the Off-center sluggish cell illustrated in Fig. 2*C*. Cells of this type were identified by their characteristically weak responses at the end of a light pulse (24) and the relatively prolonged time course of the spike-triggered average stimulus. They comprised ≈5% of recorded ganglion cells (see also ref. 24). APB failed to alter the receptive fields of each of 10 Off-center sluggish cells in nine retinas. Another type of cell, not yet characterized but clearly distinct from On–Off DS and Off sluggish cells, also continued to respond to the stimulus in the presence of APB. This type of cell comprised ≈5% of all recorded ganglion cells. The remaining Off-center ganglion cells responded briskly after a light stimulus. APB dramatically reduced or eliminated the responses of these cells to dim light. Results similar to those illustrated in Fig. 2 were observed in four retinas exposed to higher concentrations of APB (60–100 μM) and in two additional retinas tested with light stimuli 2- to 4-fold dimmer than the 0.96 $Rh^*{\cdot}rod^{-1}{\cdot}s^{-1}$ mean intensity used in the experiment of Fig. 2.

It seems unlikely that ganglion cell responses persisted in APB due to incomplete block of the rod to RDB cell synapse. APB blocked the light responses of all On-center ganglion cells

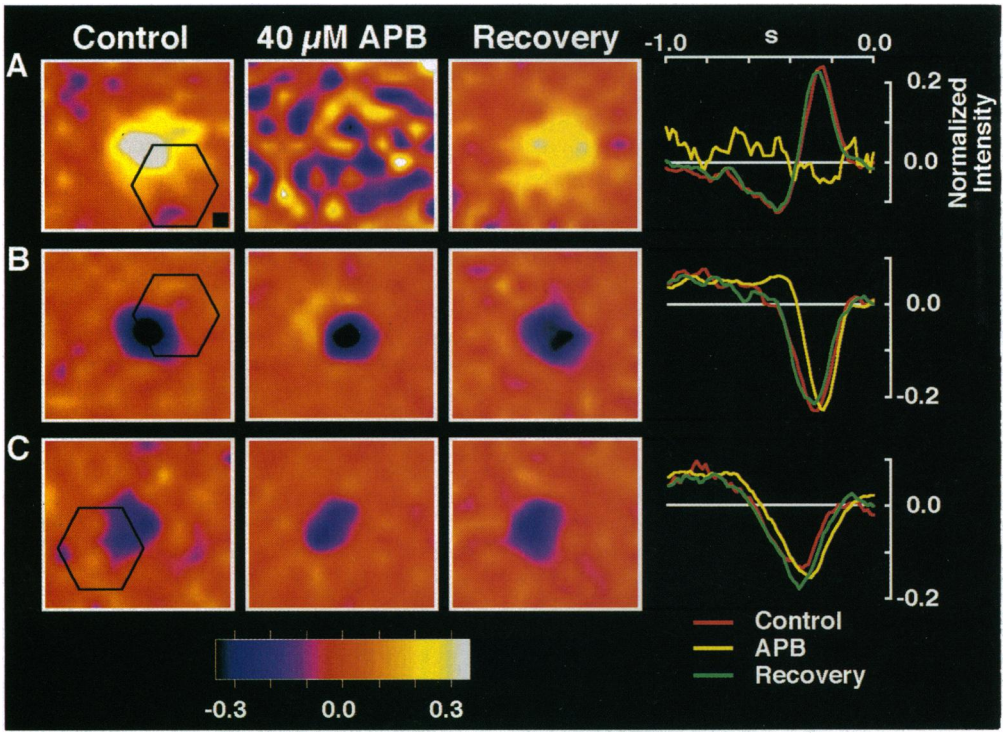

FIG. 2. Effect of APB on ganglion cell receptive fields. (*A*) Results from an On-center brisk cell. (*B*) On–Off DS cell. (*C*) Off-center sluggish cell. Receptive fields were measured by applying a dim, randomly varying checkerboard to the photoreceptor layer and subsequently computing the average stimulus intensity, a function of space and time, that preceded a spike. (*Left*) Spatial profiles of the receptive fields at a time near the peak of the temporal spike-triggered average stimulus, using pseudocolor format. (*Right*) Time course of spike-triggered average over the center of the receptive field. Intensity axis for the plots on both the left and right is normalized such that +1 and −1 correspond to the high and low intensities in the checkerboard, with the time-averaged normalized intensity being zero (17). Absolute intensity varied between 0 and 1.92 $Rh^*{\cdot}rod^{-1}{\cdot}s^{-1}$, with the mean being 0.96 $Rh^*{\cdot}rod^{-1}{\cdot}s^{-1}$. Hexagons show position of the borders of the electrode array; solid square in top left field shows relative size of one element in the checkerboard. Spatial receptive fields were smoothed by cubic spline interpolation. APB concentration was 40 μM. Refresh rate for the checkerboard was 16.7 Hz.

under both scotopic and photopic conditions (36 cells in three retinas stimulated with pulses of light and >200 cells stimulated with the flickering checkerboard). Although APB completely suppressed firing in many of the On-center cells, it might be argued that hypothetical subthreshold light responses persisted, but against this notion is the observation that six On-center cells continued to fire in APB yet did not respond to light. Furthermore, the light responses that persisted in APB

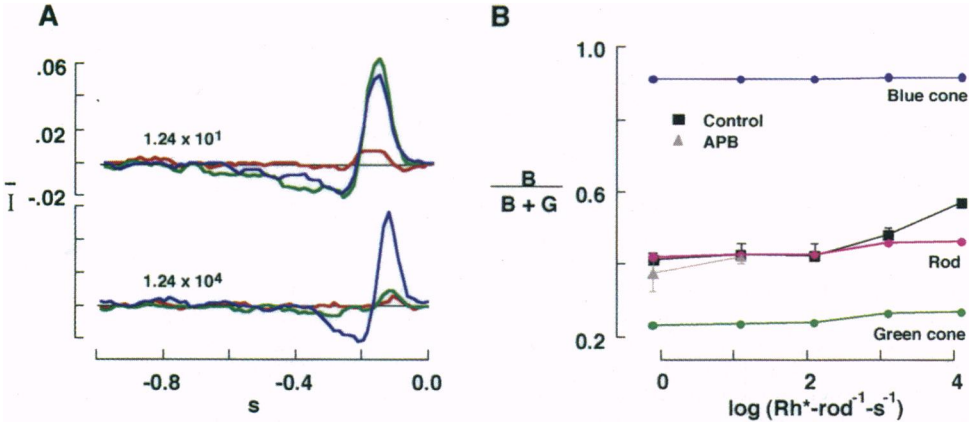

FIG. 3. Evidence that at low light levels the APB-resistant input to ganglion cells originated in rods. (*A*) Spectral properties of an On-center ganglion cell in the inferior retina at scotopic (*Upper*) and photopic (*Lower*) intensities. Receptive fields were characterized with a polychromatic checkerboard. Spike-triggered average stimuli were calculated for each phosphor on its own. Normalized intensities, $\bar{I}$, of the three phosphors in the receptive field center are shown as functions of time. (*B*) Spectral properties of ganglion cells at several mean stimulus intensities. For each cell, the ratio of normalized phosphor intensities was calculated at the peak of the time course as $B/(B + G)$ where B and G are the blue and green phosphor intensities, respectively; the contribution of the red phosphor was negligible. Squares, results from six ganglion cells (mean ± SD; five Off-center and one On–Off DS cell). Triangles, results from a subset of the cells in 40 μM APB (three cells near 1.0 $Rh^*{\cdot}rod^{-1}{\cdot}s^{-1}$, mean and range; five cells at 12.4 $Rh^*{\cdot}rod^{-1}{\cdot}s^{-1}$, mean ± SD). Additional cells recorded during this experiment were not plotted because their spikes could not be identified at all intensities. In particular, a total of five On–Off DS cells were identified in control and APB-containing solutions at a mean stimulus intensity of 12.4 $Rh^*{\cdot}rod^{-1}{\cdot}s^{-1}$ as well as at the brightest stimulus intensity. Ratios for these cells (mean ± SD) were as follows: dim control, 0.45 ± 0.03; dim APB, 0.44 ± 0.01; bright control, 0.58 ± 0.02. Predicted ratios for inputs originating in blue cone, rod, and green cone pigments are shown (21); they vary slightly with intensity due to variations in the spectral attenuation of the neutral density filters. Results in *A* and *B* were obtained from different preparations. Larger blue shift in *A* may be attributable to regional variation in the retina.

were apparently not mediated by the RDB–AII amacrine cell pathway: Off-center sluggish and On–Off DS cells continued to respond to dim light in 10 μM strychnine or 10 μM strychnine with 40–50 μM APB. At 10 μM, strychnine should completely block the glycine receptors that mediate synaptic transmission between AII amacrine and cone hyperpolarizing bipolar cells (see Fig. 1) (1, 25, 26).

The spectral sensitivity of the APB-resistant pathway confirmed that it originated in rods rather than cones. Spectral measurements were made in a region of the inferior retina with a high density of blue cones (27). Unlike green cones, these cells have an absorption spectrum that is well separated from the rod spectrum. Fig. 3*A* illustrates how the spectral sensitivity of an On-ganglion cell changed when cones took over from rods. In Fig. 3*A Upper*, the stimulus produced an average of 12.4 $Rh^*{\cdot}rod^{-1}{\cdot}s^{-1}$, and the relative effectiveness of the blue and green phosphors was well predicted by the Dartnall nomogram for rhodopsin absorption (20). In Fig. 3*A Lower*, the mean stimulus intensity was increased 1000-fold. Here the increased relative effectiveness of the blue phosphor was consistent with pure blue cone input. This spectral shift was used to determine the light intensity at which cones began to contribute to a ganglion cell's response. Fig. 3*B* plots the relative effectiveness of the blue phosphor as a function of stimulus intensity for six simultaneously recorded Off-center and On–Off DS ganglion cells. The effectiveness of the blue phosphor was consistent with pure rod input when the monitor produced $<100\ Rh^*{\cdot}rod^{-1}{\cdot}s^{-1}$. The increased effectiveness of the blue phosphor at intensities $>1000\ Rh^*{\cdot}rod^{-1}{\cdot}s^{-1}$ indicated increasing blue cone input. APB-resistant signaling was typically studied at intensities $<10\ Rh^*{\cdot}rod^{-1}{\cdot}s^{-1}$. Furthermore, if cone signals drove the ganglion cells in APB, the blue phosphor's effectiveness should be close to that observed in bright light. Instead, it was consistent with pure rod input.

The failure of APB to block rod input to On–Off DS and Off-center sluggish ganglion cells (Fig. 2) was confirmed by measurements of dark-adapted response–intensity relations (Fig. 4*A*). APB had little effect on response–intensity relations of On–Off DS and Off-center sluggish cells (open symbols), while it abolished responses in the On-center cell whose relation in control solution is plotted by solid circles. Table 1 collects results from several cells of each type as well as from a single Off-center brisk cell in this preparation. APB also failed to affect the response–intensity relations of six On–Off DS and three Off-center sluggish cells in three other preparations.

Table 1. Effect of APB on response–intensity relations

	Control, $K_{1/2}$ ($Rh^*{\cdot}rod^{-1}{\cdot}s^{-1}$)	APB, $K_{1/2}$	N
On brisk	0.59 ± 0.16		3
Off brisk	0.3	1.92	1
On–Off DS	1.49 ± 0.27	1.31 ± 0.25	4
Off sluggish	1.49 ± 0.57	1.19 ± 0.52	3

Collected results (means ± SD) are from the preparation of Fig. 4*A*. One On-center brisk cell that had a >5-fold higher $K_{1/2}$ in control was excluded. Spikes from two On–Off DS cells were observed in control but not during subsequent runs. N is number of cells.

The results in Fig. 4*A* suggest that On–Off DS and Off-center sluggish cells received little if any input from the RDB–AII amacrine cell pathway. The conclusion is supported by the results in Fig. 4*B*. In this experiment, the retina was continuously stimulated with a flickering random checkerboard, producing a steady stream of spikes from each ganglion cell. The spike rate is plotted as a function of time before, during, and after application of APB. APB abolished firing in the On-center brisk cell and accelerated firing in the Off-center brisk cell. These are the effects expected for a large APB-induced hyperpolarization of RDB cells transferred to the AII amacrine cells and then to ganglion cells by sign-preserving and sign-reversing connections, respectively (see Fig. 1). Similar results were obtained in cat retina (1). However, APB had little effect on the simultaneously recorded activity of the On–Off DS and Off sluggish cells, suggesting that these cells did not receive significant input from AII cells.

DISCUSSION

The isolated rabbit retina proved well suited for study by multielectrode array recording. It gave stable light responses for many hours and was accessible for pharmacological manipulation. Multiple cells could be recorded simultaneously in a single preparation, allowing simple, direct comparisons of response properties and sensitivity to drugs.

The finding that rod signals reached On–Off DS and Off-center sluggish ganglion cells with transmission to the RDB cells blocked provides direct evidence that rod signals can reach ganglion cells over a pathway not involving RDB and AII amacrine cells. It seems most likely that in the alternative pathway rod signals flow through gap junctions to cones and from cones to the inner retina over cone bipolar cells. Evi-

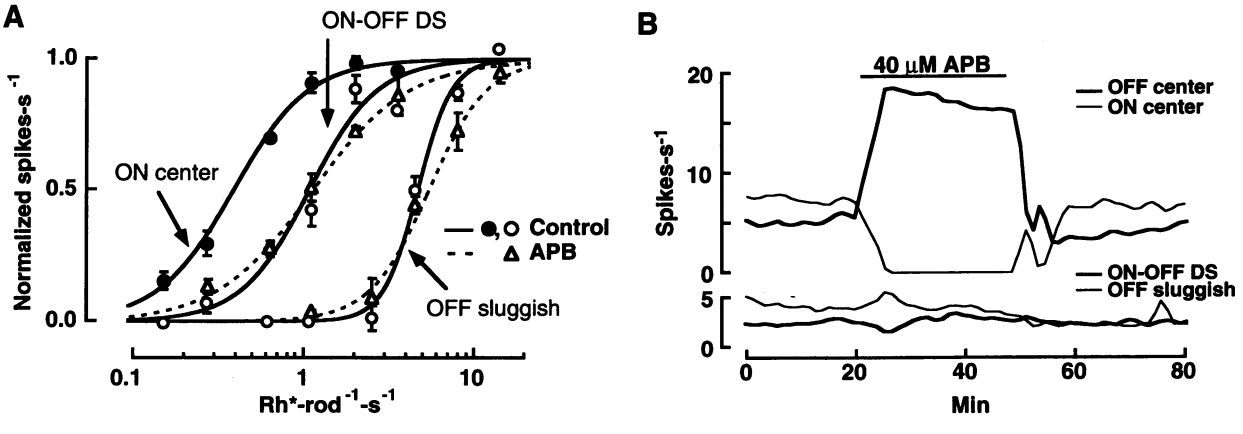

FIG. 4. (*A*) Response–intensity relations of three ganglion cells in control solution and in 40 μM APB. Increase in firing rate produced by 0.5-s pulses of light is plotted against intensity. Curves are least-squares fits to the equation $R = R_{max}I^n/(I^n + K_{1/2}^n)$, where R is the mean increase in spike rate following a pulse of intensity I, R_{max} is the maximal response, n is a steepness coefficient, and $K_{1/2}$ is the intensity that produces a half-maximal increase in rate. The experimental relation for the Off sluggish cell has been displaced to the right on the abscissa by 0.6 log unit for clarity. Maximum increases in firing rate ($spikes{\cdot}s^{-1}$) were 24.4 (On-center control), 12.5 and 15.5 (On–Off DS; control and APB), and 21.5 and 20.0 (Off-center sluggish; control and APB). (*B*) Mean spike rate plotted against time for four ganglion cells before, during, and after exposure to 40 μM APB. Retina was stimulated continuously with a green/black checkerboard pattern producing a mean of 4.2 $Rh^*{\cdot}rod^{-1}{\cdot}s^{-1}$.

dence for the functional importance of the gap junctions between mammalian rods and cones has been obtained by recording rod responses in cones (12, 14) and cone-driven horizontal cells (11–13). Alternatively, rod signals may reach the inner retina over a hyperpolarizing rod bipolar cell (28, 29). Against this possibility, anatomical observations indicate that mammalian rods contact a single class of bipolar cell whose axon terminates in the On-lamina of the inner plexiform layer (3, 30, 31). Moreover, only depolarizing responses have been observed in recordings from rabbit rod bipolar cells (32).

Since individual cones are thought to contact nearly all types of cone bipolar cells (33), one might expect a rod–cone pathway to distribute signals to all ganglion cells. Indeed, strong rod stimuli elicited weak responses in Off-center brisk cells in APB. These responses were superimposed on a high tonic firing rate that presumably resulted from removal of inhibition exerted by AII amacrine cells. An unexpected finding was that rod-driven Off responses persisted unaltered in On–Off DS and Off-center sluggish ganglion cells. The implication is that rod-driven Off responses in these cells were mediated exclusively by cone bipolar cells that are not postsynaptic to AII amacrine cells. Little is known about the axonal junctions of cone bipolar cells in rabbit retina (see ref. 34). In cat retina, however, ultrastructural studies suggest that one class of depolarizing cone bipolar cell does not receive gap junctional contacts from AII cells (33). Interestingly, this wide-field bipolar cell selectively contacts ganglion cells outside of the α/Y and β/X classes.

It has been suggested that rod–cone coupling operates at mesopic rather than scotopic intensities (2, 10, 11), yet we found that the APB-resistant pathway operated at stimulus intensities that were 1–2 log units dimmer than those that elicited ganglion cell responses via blue cones. Indeed, the APB-resistant pathway appeared to function at mean stimulus intensities as low as 0.2 $Rh^*{\cdot}rod^{-1}{\cdot}s^{-1}$. This intensity is $\approx$10-fold lower than that at which rod–cone transmission has been observed in cat retina by monitoring the responses of interneurons (11, 12). Similarly, recordings from cones in the monkey retina suggest that rod–cone transmission is significant only for rod responses larger than $\approx$5 mV, which would require a steady excitation of >15 $Rh^*{\cdot}rod^{-1}{\cdot}s^{-1}$ (14). Perhaps coupling in the rabbit retina is stronger than in these other species.

In summary, we have obtained evidence that an alternative pathway transmits signals to ganglion cells in parallel with the classical RDB cell pathway. This alternative pathway mediated ganglion cell responses to lights as dim as 0.2 $Rh^*{\cdot}rod^{-1}{\cdot}s^{-1}$. Moreover, while RDB cells seem to carry rod input to briskly responding ganglion cells, the alternative path apparently provides the dominant route for rod signals to reach Off-center sluggish and directionally selective ganglion cells. In the alternative pathway, signals presumably flow from rods to cones via electrical junctions and then to the inner retina via cone bipolar cells.

We thank Robert Schneeveis for excellent technical assistance. This work was supported by National Institutes of Health Grant EY05750 (D.A.B.), the Ruth and Milton Steinbach Fund (D.A.B.), National Institutes of Health Postdoctoral Fellowship EY06387 (S.H.D.), and a fellowship from The Bank of America–Giannini Foundation (S.H.D.).

1. Müller, F., Wässle, H. & Voigt, T. (1988) *J. Neurophysiol.* **59,** 1657–1672.
2. Daw, N. W., Jensen, R. J. & Brunken, W. J. (1990) *Trends Neurosci.* **13,** 110–115.
3. Strettoi, E., Dacheux, R. F. & Raviola, E. (1990) *J. Comp. Neurol.* **295,** 449–466.
4. Vaney, D. I., Young, H. M. & Gynther, I. C. (1991) *Vis. Neurosci.* **7,** 141–154.
5. Slaughter, M. M. & Miller, R. F. (1981) *Science* **211,** 182–185.
6. Shiells, R. A., Falk, G. & Naghshineh, S. (1981) *Nature (London)* **294,** 592–594.
7. Nawy, S. & Jahr, C. E. (1991) *Neuron* **7,** 677–683.
8. Dolan, R. P. & Schiller, P. H. (1989) *Vis. Neurosci.* **2,** 421–424.
9. Raviola, E. & Gilula, N. B. (1973) *Proc. Natl. Acad. Sci. USA* **70,** 1677–1681.
10. Smith, R. G., Freed, M. A. & Sterling, P. (1986) *J. Neurosci.* **6,** 3505–3517.
11. Steinberg, R. H. (1969) *Vision Res.* **9,** 1319–1329.
12. Nelson, R. (1977) *J. Comp. Neurol.* **172,** 109–136.
13. Dacheux, R. F. & Raviola, E. (1982) *J. Neurosci.* **2,** 1486–1493.
14. Schneeweis, D. M. & Schnapf, J. L. (1995) *Science* **268,** 1053–1056.
15. Conner, J. D. & MacLeod, D. I. A. (1977) *Science* **195,** 698–699.
16. Conner, J. D. (1982) *J. Physiol. (London)* **332,** 139–155.
17. Meister, M., Pine, J. & Baylor, D. A. (1994) *J. Neurosci. Methods* **51,** 95–106.
18. Reid, R. C. & Shapley, R. M. (1992) *Nature (London)* **356,** 716–718.
19. Baylor, D. A. & Hodgkin, A. L. (1973) *J. Physiol. (London)* **234,** 163–198.
20. Dartnall, H. J. A. (1953) *Br. Med. Bull.* **9,** 24–30.
21. Baylor, D. A., Nunn, B. J. & Schnapf, J. L. (1987) *J. Physiol. (London)* **390,** 145–160.
22. Meister, M., Wong, R. O. L., Baylor, D. A. & Shatz, C. J. (1991) *Science* **252,** 939–943.
23. Barlow, H. B., Hill, R. M. & Levick, W. R. (1964) *J. Physiol. (London)* **173,** 377–407.
24. Caldwell, J. H. & Daw, N. W. (1978) *J. Physiol. (London)* **276,** 257–276.
25. Suzuki, S., Tachibana, M. & Kaneko, A. (1990) *J. Physiol. (London)* **421,** 645–662.
26. Karschin, A. & Wässle, H. (1990) *J. Neurophysiol.* **63,** 860–876.
27. Juliusson, B., Bergström, A., Rölich, P., Ehinger, B., van Veen, T. & Szél, A. (1994) *Invest. Ophthalmol. Visual Sci.* **35,** 811–818.
28. Nelson, R., Kolb, H., Famiglietti, E. V., Jr. & Gouras, P. (1976) *Invest. Ophthalmol. Visual Sci.* **15,** 946–953.
29. Nelson, R. & Kolb, H. (1983) *Vision Res.* **23,** 1183–1195.
30. Dowling, J. E. & Boycott, B. B. (1966) *Proc. R. Soc. London B* **166,** 80–111.
31. Boycott, B. B. & Dowling, J. E. (1969) *Philos. Trans. R. Soc. London Ser. B* **255,** 109–184.
32. Dacheux, R. F. & Raviola, E. (1986) *J. Neurosci.* **6,** 331–345.
33. Cohen, E. & Sterling, P. (1990) *Philos. Trans. R. Soc. London Ser. B* **330,** 305–321.
34. Famiglietti, E. V., Jr. (1981) *Vision Res.* **21,** 1559–1563.